



## Research on the Flow Characteristic in a Multi-Stage Multiphase Pump by Numerical Simulations

Y. Shi<sup>1,2†</sup> and H. W. Zhu<sup>3</sup>

<sup>1</sup> School of mechanical engineering, Beijing Key Laboratory of Pipeline Critical Technology and Equipment for Deepwater Oil & Gas Development, Beijing Institute of Petrochemical Technology, Beijing, 102617, China

<sup>2</sup> Beijing academy of safety engineering and technology, Beijing, 102617, China

<sup>3</sup> College of Mechanical and Transportation Engineering, China University of Petroleum, Beijing, 102249, China

†Corresponding Author Email: shiyi@bipt.edu.cn

(Received May 10, 2020; accepted August 7, 2020)

### ABSTRACT

As a cost-effective option for subsea gas and oil fields development, multiphase pump has been widely used and plays an important role in promoting field production especially for those brownfields. The objective of this research is to study the variations of flow parameters at the inlet of each stage in a five-stage helico-axial pump under design conditions by using commercial CFD packages. The numerical results show that inlet volume flow rate, gas volume fraction (GVF) and flow angle of each stage both decreases from the first stage to the fifth stage because of the compression. The variations of these parameters along the flow direction are susceptible to the effect of rotational speed and initial gas volume fraction at inlet of the first stage. These inlet flow parameters from inlet to outlet of the five-stage pump just change little when the initial inlet GVF is lower than 10% or higher than 90%. While the variation is obvious when inlet GVF is from 20% to 80%. Based on numerical simulation results, the stage-by-stage design method is proposed and geometry parameters such as inlet impeller hub diameter and inlet angle of blade in the second stage are modified according to its inlet flow conditions. The comparison results between the modified pump and original pump show that pressure distribution at leading edge of impeller blades in each stage becomes uniform in the modified multistage pump. The inlet incident flow loss of each stage is diminished and internal flow conditions has been significantly improved. Thus, the pump's boosting capacity is enhanced. These research results in this paper are instructive for the performance optimization of multistage pumps used in gas oil fields.

**Keywords:** Multiphase pump; Numerical simulation; Gas-liquid flow; Stage-by-stage design; Subsea boosting.

### NOMENCLATURE

$A$	cross-sectional area	$V_c$	radial velocity
$CFD$	computational fluid dynamics	$w$	angular velocity
$d_h$	hub diameter		
$D_t$	impeller shroud diameter	$\beta_0$	inlet flow angle
$ESP$	electrical submersible pump	$\beta_s$	inlet angle at impeller on shroud
$GVF$	gas volume fraction	$\beta_h$	inlet angle impeller on hud
$h_r$	hub ratio of inlet	$\beta$	inlet angle
$H$	head per stage	$\Delta\beta$	incident angle
$n$	rotational speed	$\rho_L$	liquid density
$Q$	volume flow rate	$\rho_g$	gas density
$r$	radius		
$SST$	shear stress transport		
$V_m$	axial velocity		

## 1. INTRODUCTION

Multiphase pumps are widely used in subsea gas oil field production nowadays. By the application of multiphase boosting technology, cost of processing facilities could be reduced. Besides, the back pressure of wellhead in gas oil field can be decreased and the long-distance transportation of gas-oil can be achieved, as well as extension of the field lifetime. The common multiphase pumps can be classified according to working principle as rotodynamic or positive displacement pumps. Typical rotodynamic multiphase pumps are centrifugal, semi-axial (Zhu *et al.* 2018a, 2018b) and helico-axial (Gié *et al.* 1992) pumps. While the positive displacement pumps mainly include twin-screw pumps (Vetter *et al.* 2000), progressive cavity pump (Mirza *et al.* 1997) and so on. Among them, helico-axial pumps dominate the market in multiphase pumping systems for subsea applications (Nunez *et al.* 2016). The existence of gas is a critical factor that leads to degradation of pump performance (Gülich 2014), which also affects the variations of gas-liquid flow characteristics in each stage for a multistage pump. Some researches have been made to investigate the two-phase flow characteristic and influence of stage number on performance in a multiphase pumps. De Sails *et al.* (1996) pointed out that the gas volume flow rate decreases through a multi-stage pump because of the compression. Therefore, the pump is generally equipped with different series of geometries, whereby one series would have identical compression stages. The changing geometry from one series to the next provides adjustment for the decreasing volume flowrate. Cirilo (1998) studied the influence of varying number of stages for a mixed-type pump with the best-efficiency flow rate. Since the gas volume fraction (GVF) is smaller in the last few pump stages and corresponding with lower flow rates, it indicates a definite trend of less head deterioration with more stages. Pessoa *et al.* (2003) investigated the pressure changes stage by stage on a 22-stage mixed-flow-type pump under two-phase flow conditions by an experimental study. The results show that average pump behavior is significantly different from that observed per stage. The pressure increment and total hydraulic horsepower behavior is different for each stage. Barrios (2007), Gamboa (2008) and Trevisan (2009) studied the oil-air flow patterns inside a transparent electrical submersible pump (ESP) by visualization experiments. It indicated that four patterns including agglomerated bubbles, gas pocket, segregated gas and intermittent gas are identified as the inlet gas volume fraction increases on the basis of observations from high-speed camera. Barrios *et al.* (2012) studied the performance of a 13-stage multi-vane pump with high gas oil ration and viscous fluids. The results recommend to calculate the stage by stage performance as well as viscosity and gas volume for viscous multiphase flow applications. Salehi *et al.* (2013) studied the effect of stage numbers on the overall performance of a 14-stage ESP by experiments in two-phase flow conditions. The results show that the ESP stage performance deteriorates as inlet gas volume fraction increases.

The deterioration is very mild until gas volume fraction reaches to a critical value where surging occurs. After this point, the rate of deterioration becomes a function of a stage number. Zhang and Cai (2016) investigated the gas-liquid flow patterns in impellers of a three-stage helico-axial multiphase pump by visualization experiments. It shows that the flow patterns vary from isolated bubbles, bubbly flow, gas pocket flow and segregated gas flow as inlet gas volume fraction increases. The size of gas pocket area decreases from the first stage to the third stage due to the compressibility of gas in the gas pocket flow condition. Shi *et al.* (2017) investigated the variations of condition parameters such as pressure, volume flow rate, gas volume fraction and inlet flow angle of impeller in each stage of a three-stage helico-axial pump by numerical simulations. The maximum rotation speed in the numerical simulation is just 3600 rpm, which is not the design parameter of pump and the speed is not high. The pump stage number is not more enough to reflect the trend of its influence on the variation of flow parameters in a multistage pump. Zhang *et al.* (2018) studied the variational characteristics of flow parameters for each impeller at different operating conditions in a five-stage helico-axial pump by numerical simulations. The maximum volume flow rate and rotational speed are 47 m<sup>3</sup>/h and 2700 rpm separately, which are both not under the design conditions.

It is obvious to find that most of current studies refer to the variations of flow parameters under two-phase flow conditions are focus on multistage electrical submersible pumps. Few researches are about helico-axial pumps and the related flow conditions are not under design parameters among those researches, which are not able to show the flow characteristic in a multistage pump comprehensively. Therefore, in this paper the variations of flow parameters such as volume flow rate, gas volume fraction, inlet flow angle and pressure in each stage of a five-stage helico-axial pump under design conditions are investigated by numerical simulations with high rotational speeds and volume flow rates. And then the stage-by-stage design of a five-stage pump under two-phase flow conditions is implemented by modifying the geometry of each stage according to the corresponding design parameters, aiming to improve the multiphase pump performance.

## 2. NUMERICAL SIMULATION METHODOLOGY

A multi-stage multiphase pump consists several compression units. Each compression unit is made of an impeller (rotating part) and a diffuser (stationary part). There are 4 blades in impeller and 11 blades in diffuser in the investigated multiphase pump. Table 1 shows the design parameters of the pump. The pictures of impeller and diffuser are shown in Fig. 1. The three-dimensional model of impeller and diffuser are built by ANSYS BladeGen, separately. The assembly of five compression units used in the numerical simulation is shown in Fig. 2. It is the fluid

flow domain part. In order to make sure the flow at inlet and outlet of pump are stable, there are extra inlet and outlet extend parts in the assembly.

**Table 1 Design parameters of the multiphase pump**

Parameters	Value
volume flow rate $Q$ (m <sup>3</sup> /h)	100
rotational speed $n$ (r/min)	4500
head per stage $H$ (m)	20
Liquid density $\rho_L$ (kg/m <sup>3</sup> )	1000
Gas density $\rho_g$ (kg/m <sup>3</sup> ) (standard condition)	1.297



(a)



(b)

**Fig. 1. Pictures of the compression unit. (a) Impeller, (b) Diffuser.**

The mesh of impeller and diffuser in the assembly are generated by ANSYS Turbogrid 17.2 while that of the inlet and outlet extend parts are generated by ANSYS ICEM. They are both structured hexahedral grids with high quality. Figure 3 shows the mesh of single flow passage in impeller and diffuser. The Euler-Euler multiphase flow model is applied in the numerical simulation. Specifically, the inhomogeneous multiphase model is used, which refers to the case where separate velocity fields and other relevant fields

exist for each fluid. The pressure field is shared by all fluids. The fluids interact by interphase transfer terms and particle models is used. For water phase, the shear stress transport (SST) k-omega turbulence model is used. While for gas phase, the dispersed phase zero equation turbulence model is used. The velocity is defined as the pump inlet condition and the values of gas volume fraction and water volume fraction are both given. The sum of gas volume fraction and water volume fraction is equal to 1. For the outlet condition, the value of static pressure is given. For the walls such as shroud and hub of impellers, the no-slip velocity condition is imposed. Interfaces between impeller and diffuser in each stage are set using the frozen-rotor technique while the stage-average method is applied to interfaces between other domains. The convergence residual is set as  $1e^{-6}$  to ensure the numerical simulation is convergent. The time step for the iterative calculation is set as auto timescale which means the time step varies in the simulation process.

Grid independence verification was made for one compression unit under single phase flow condition. The inlet volume flow rate is 100 m<sup>3</sup>/h and rotational speed is 3000 rpm. The verification details were shown in reference (Shi *et al.* 2018). Final grid number of impeller, diffuser, inlet and outlet extend regions are 452568, 536877, 46800 and 90882 respectively. So grid number of one-stage is 1127127 and it is 5084907 for the whole five-stage. In CFD simulations, some conservation equations should be solved. In this study, the isothermal condition is applied to fluid flow domain. The temperature is set to be the same as ambient temperature. Since the gas medium is air ideal gas, the density changeable is considered. The energy conservation equation can be ignored and no source or diffusion terms appear in the mass balances. The mass and momentum equations of fluid can be found in ANSYS official tutorial (ANSYS 2016). As to the validation of numerical simulation method, the details are shown in reference (Shi *et al.* 2018), which are not shown here again.

### 3. NUMERICAL SIMULATION RESULTS AND ANALYSIS

Due to the compressibility of gas, the gas volume flow rate decreases through a multi-stage pump by compression. Some other parameters such as pressure and gas volume fraction also vary at the inlet of each stage. In the following part, variations of inlet flow parameters in every compression unit are investigated comprehensively.

#### 3.1 Flow Characteristic in Each Stage Under the Same flow Condition

The inlet flow parameters of each stage such as volume flow rate, gas volume fraction, relative flow angle are analyzed with the flow condition that inlet volume flow rate is 100 m<sup>3</sup>/h, inlet gas volume fraction is 30% and rotational speed is 4500 r/min. Distributions of pressure and gas volume fraction in impeller and diffuser are also studied.



Fig. 2. Geometry of the compression units in the five-stage helico-axial multiphase pump.

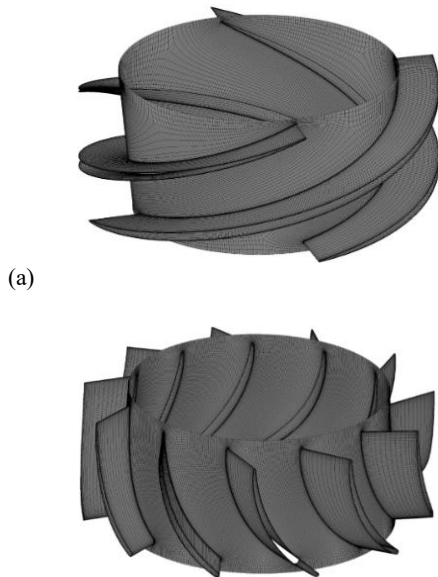


Fig. 3. The hexahedral grids of impeller and diffuser. (a) Impeller, (b) Diffuser.

### 3.1.1 Variations of flow Parameters in Each Stage

The main inlet flow parameters of each stage are volume flow rate, gas volume fraction, axial velocity, and inlet flow angle of blade on impeller shroud. The axial velocity  $V_m$  is related to volume flow rate  $Q$  and cross-sectional area of the inflowing flow path  $A$ .  $V_m$  can be calculated from Eq. (1) and Eq. (2). The radial velocity is  $V_c$ . It is calculated from Eq. (3). Then the inlet flow angle of blade  $\beta_0$  is defined in Eq. (4) with axial velocity and radial velocity based on the velocity triangle theory (Brennen 2011).

$$V_m = \frac{Q}{A} \quad (1)$$

$$A = \frac{\pi(D_t^2 - d_h^2)}{4} \quad (2)$$

$$V_c = r \times \omega \quad (3)$$

$$\beta_0 = \tan^{-1} \frac{V_m}{V_c} \quad (4)$$

Where  $D_t$  and  $d_h$  refer to the inlet impeller shroud diameter and hub diameter respectively,  $r$  refers to the radius,  $\omega$  refers to the angular velocity. The inlet

angle of blade  $\beta$  is the sum of flow angle of blade  $\beta_0$  and incident angle  $\Delta\beta$ . Variations of these main parameters are shown in Table 2. It can be seen from Table 2 that inlet gas volume fraction decreases from the first stage to the fifth stage, as well as the gas-liquid volume flow rate and the inlet flow angle of blade on impeller shroud. In order to reflect the variation trend more directly, the curves of inlet gas volume fraction and volume flow rate along the flow direction are shown in Fig. 4. The two parameters decrease rapidly in the first two stages and then decrease smoothly from the fourth stage to the fifth stage. It indicates that the compressibility gradually decreases as gas in the gas-liquid phase is compressed along the five multi-stage pump.

Table 2 Inlet flow parameters at each compression unit

Number of stage	GVF (%)	Axial velocity (m/s)	Volume flow rate (m <sup>3</sup> /h)	Inlet flow angle (°)
1	30	3.78	100	6.78
2	23.6	3.60	91.63	6.46
3	19.9	3.48	87.46	6.24
4	16.6	3.37	83.97	6.04
5	14.5	3.26	81.90	5.85

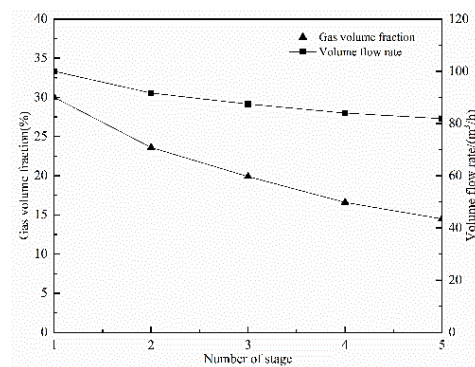


Fig. 4 Variations of inlet GVFs and flowrates at each stage.

### 3.1.2 Variations of Internal flow Field in Each Stage

#### (1) Pressure Distributions

The pressure distribution through flow direction on each compression unit on the blade-to-blade plane is



Fig. 5 Pressure distribution on the blade-to-blade plane at the mid-span surface.

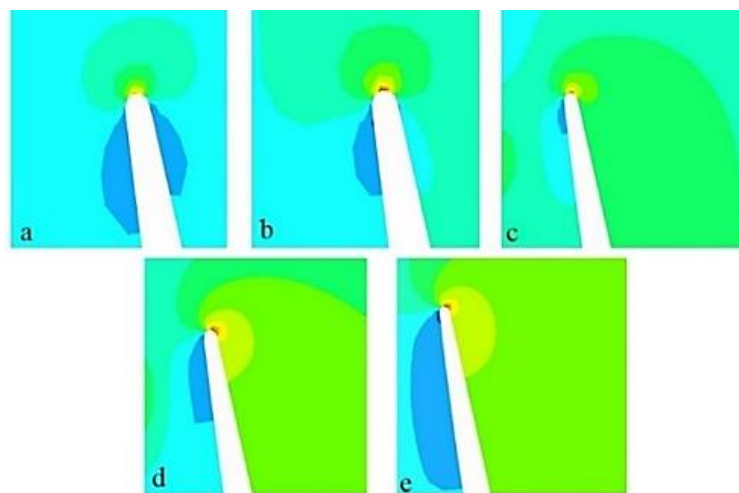


Fig. 6 Pressure distribution on the area of leading edge in blade on blade-to-blade plane.

shown in Fig. 5. Pressure increases gradually from inlet to outlet. To show the difference of pressure distribution precisely at certain area on impeller blade, the part of leading edge on impeller blade in each stage is enlarged and pressure distributions are shown separately in Fig. 6. It can be seen that there are some differences for pressure distribution on the suction side and pressure side of impeller blade among the five stages. The pressure is almost symmetrical on two sides of impeller blade in the first stage and maximum pressure occurs on the top of the leading edge. On the second stage, maximum pressure is also on the top point. But pressure difference occurs on two sides of impeller blade. The value of pressure on pressure side is higher than that of the suction side. While from the third stage to the fifth stage, maximum pressure point on that area gradually moves from the top of leading edge to the pressure side. And the pressure difference between pressure side and suction side of impeller blade on the given area becomes more apparent.

The reason which causes difference of pressure distribution on leading edge at each stage is related to the inlet angle of blade and corresponding flow

conditions. Geometry parameters of impeller such as inlet flow angle in the first stage are consistent to the design parameters such as inlet volume flow rate. The attack angle is also suitable which obtain there is no pressure difference between the pressure side and suction side at the leading edge of impeller blade in the first stage. Since the volume flow rate decreases from the second to the fifth stage, the relative flow angle also decreases. While all the geometry parameters including the inlet angle of blade are the same as those of the first stage, the inlet incident angle and incident flow loss at the impeller blade become to increase in the following compression units. As a result, pressure difference occurs between two sides of the impeller blade. Thus, the performance of following stages is affected. In order to improve the flow condition and diminish the incident flow loss at impeller inlet in each stage, the inlet angle of blade should be modified in each stage.

## (2) Gas Volume Fraction Distribution

Gas and liquid in two-phase flow are subjected to centrifugal force in the rotodynamic pump. Since the

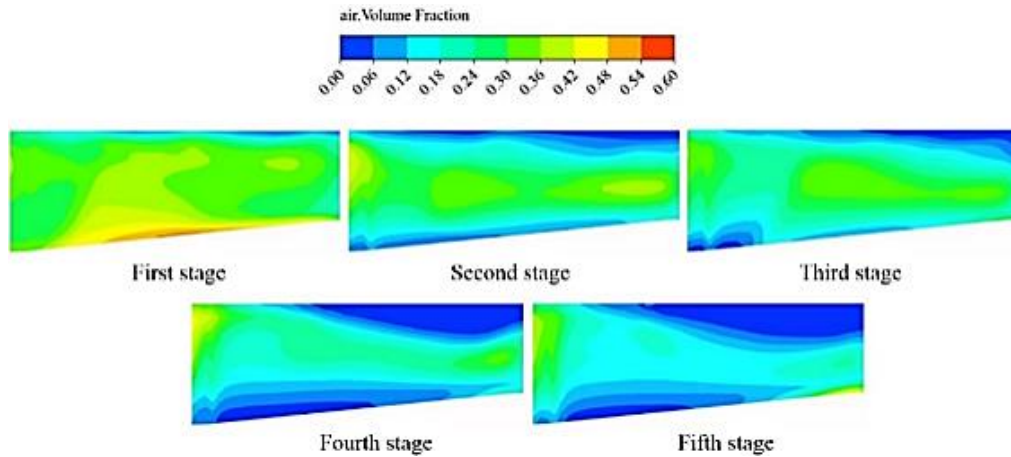


Fig. 7. Gas distribution on the meridional plane of blade at each stage.

density of gas is much smaller than that of liquid, gas is easily concentrated to the central part along the radial direction. Figure 7 shows the distribution of gas volume fraction on the meridional plane of impeller blade in each stage. The inlet gas volume fraction in the first stage is 30%. Gas concentration area occurs at the middle part near the impeller hub in the first stage. The maximum value of gas volume fraction is about 60%. On the meridional plane of the following stages, gas volume fraction and the gas concentration area both decrease due to the degree of compression increases.

### 3.2 Flow Characteristic in Each Stage Under Different Flow Conditions

Flow characteristic of each stage under the same flow conditions have been analyzed. And the results show that the parameters such as gas volume fraction, pressure and relative flow angle vary along the flow direction from the first stage to the fifth stage. In the following part, influence of different flow conditions on the variation trend of flow parameters are investigated.

#### 3.2.1 The Effect of Rotational Speed

The effect of rotational speed on variations of inlet gas volume fraction and relative flow angle at impeller shroud from the first stage to the last stage are investigated. In the numerical simulation, the inlet volume flow rate is 100 m<sup>3</sup>/h, inlet gas volume fraction is 30% and rotational speeds are 3500r/min, 4000 r/min and 4500 r/min respectively. Figure 8 shows the variations of inlet gas volume fraction in each stage. The value decreases rapidly in the first two stages and becomes steady in the last three stages when rotational speeds are 3500 r/min and 4000 r/min. When the rotational speed increases to 4500 r/min, the value of gas volume fraction keeps decreasing from the first stage to the last stage. This indicates that gas can be further compressed at higher rotational speed which contributes to the improvement of pump performance.

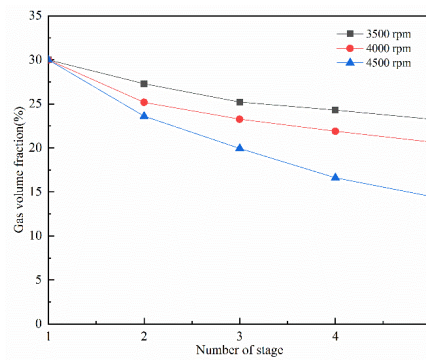


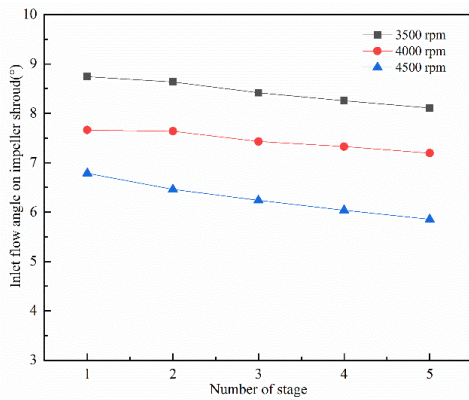
Fig. 8. Variations of inlet GVs at each stage with different rotational speeds.

Figure 9 shows the variation of flow angle at inlet impeller shroud of each stage with different rotational speeds. Although the flow angle of each stage decreases from the first stage to the fifth stage, the difference of flow angles between the first stage and the last stage are not obvious at relative low rotational speed. For example, the difference is less than 0.7 degree when rotational speeds are 3500 r/min and 4000 r/min. As rotational speed increases to 4500 r/min, the difference is about 1 degree. It indicates the significant effect of rotational speed on variations of inlet flow parameters in each stage, which has the same conclusion with that from Fig. 8.

#### 3.2.2 The Effect of Volume flow Rate

The effect of volume flow rate on inlet gas volume fraction and flow angle at impeller shroud in each stage are investigated with three different inlet volume flow rates (80 m<sup>3</sup>/h, 100 m<sup>3</sup>/h and 120 m<sup>3</sup>/h). The inlet gas volume fraction is 30% and rotational speeds is 4500 r/min. Figure 10 shows variations of inlet GVs at each stage. It decreases as the stages number increases and the three curves corresponding to different volume flow rates are similar. There are not obvious differences of the inlet GVs among three different volume flow rates in the same stage. Figure 11 shows variations of flow angle on impeller shroud at each stage with different flow rates. Since flow angle is directly related to volume flow rate, the

difference of flow angles among different volume flow rates at the same stage is obvious. It increases as the flow rate grows.



**Fig. 9. Variations of inlet flow angle on impeller shroud with different rotational speeds.**

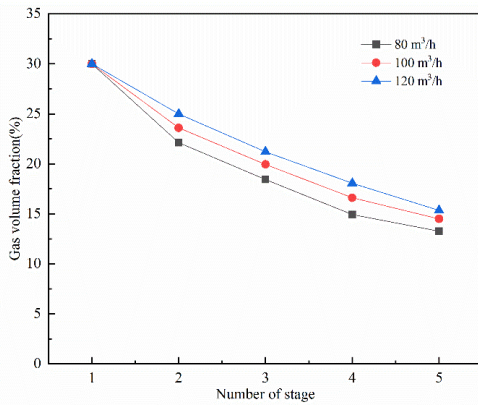


**Fig. 10. Variations of inlet GVF at each stage with different flow rates.**

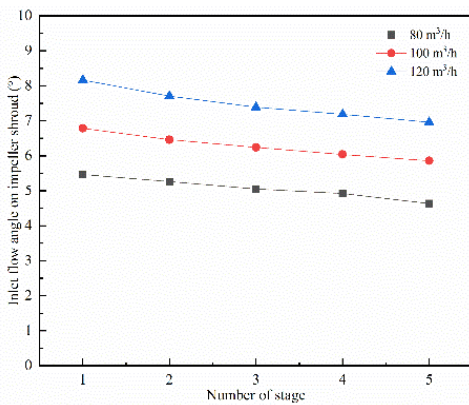


**Fig. 11. Variations of flow angle on impeller shroud at each stage with different flow rates.**

### 3.2.3 The Effect of Inlet GVFs

The variations of flow parameters with different inlet gas volume fraction ranges from 10%-90% are studied. The inlet volume flow rate is 100 m³/h and rotational speed is 4500 r/min. Figure 12 shows the

variations of inlet volume flow rate in each stage. It decreases from the first stage to the fifth stage with all ranges of inlet GVFs. But the downward trends are different as inlet GVF increases. When inlet GVF is 10%, there is small decline from the second stage to the last stage. When inlet GVF is larger than 10%, the volume flow rate decreases dramatically from the second stage to the fourth stage and varies little from the fourth stage to the last stage.

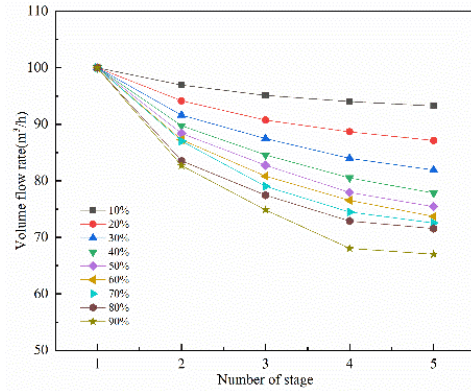


**Fig. 12. Variations of flow rates at each stage with different inlet GVFs.**

Figure 13 shows variations of GVF at the inlet of each stage when inlet GVF of pump ranges from 10%-90%. It decreases from the first stage to the third stage and keeps almost the same between the fourth stage and the fifth stage. When inlet GVFs are 10% and 90%, the variations are not obvious except in the first two stages. It can be explained that when inlet GVF is very low, the gas compressibility is weak. While when inlet GVF is very high, the gas-liquid two phase could be regarded as pure gas phase. The pump almost loses compression ability in this condition. When inlet GVFs ranges from 20%-80%, the decline from the first stage to the third stage are obvious and becomes stable in the last two stages.

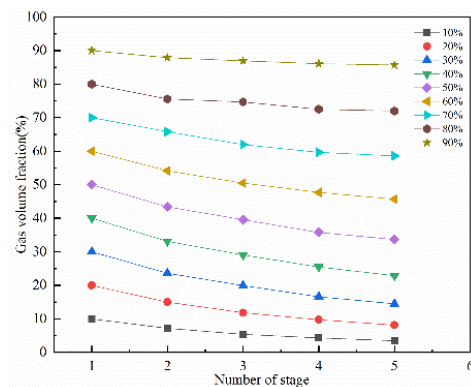


**Fig. 13. Variations of GVFs at each stage with different inlet GVFs.**

Variations of flow angle on impeller shroud at inlet of each stage with different inlet GVFs are shown in Fig. 14. It decreases rapidly along the flow direction. Curves with different inlet GVFs ranges from 40% to 70% are almost coincide with each other as the

stage number increases. When inlet GVF's are 80% and 90%, the corresponding flow angles at the first stage are obviously smaller than that with other inlet GVF's. One possible reason is that the flow is very unstable when inlet GVF becomes high. At high inlet GVF's, the flow angles of each stage decrease slowly. For example, when inlet GVF is 90%, the difference between the first stage and the fifth stage is just 0.37°.

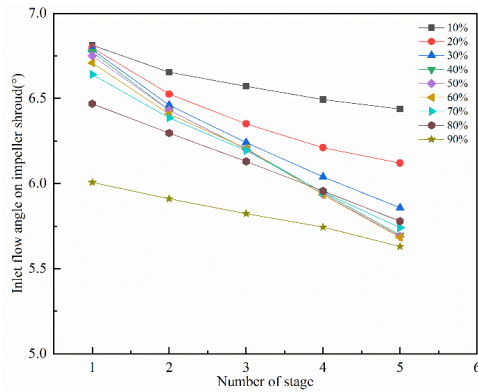


**Fig. 14. Variations of inlet flow angle on impeller shroud at each stage with different inlet GVF's.**

Based on the above analysis, rotational speed, gas volume fraction and volume flowrate both affect the inlet flow parameters of each stage. Among them, the influence of rotational speed and gas volume fraction is more obvious. With higher rotational speed such as 4500r/min, there are still apparent reduction of volume flowrate, gas volume fraction and flow angle even in the last few stages of pump since gas can be further compressed. In order to improve flow conditions at the inlet of each stage in the five-stage multiphase pump, the stage-by-stage design method is applied. When inlet GVF is very low (10%) or very high (90%), there are little changes for flow parameters at the inlet of each stage. So the stage-by-stage design method is considered according to the variation of flow parameters in each stage when inlet GVF ranges from 20%-80%.

#### 4. STAGE-BY-STAGE DESIGN OF THE MULTI-STAGE PUMP

Stage-by-stage design of a five-stage pump is conducted in this part. The second stage is redesigned firstly according to its inlet flow parameters which are from previous numerical simulation results. Since impeller is the main part of a compression unit, the focus is on determining the structural parameters of impeller. Parameters of diffuser are modified based on those of impeller.

##### 4.1 Determination of Main Geometry Parameters of Impeller

The main geometry parameters of impeller are impeller shroud diameter, impeller blade length, hub ratio of inlet, half cone angle of hub and number of blades. The hub ratio of inlet is related to inlet shroud diameter which determines the cross-sectional size

of flow passage and affects the volume flow rate. The inlet flow angle of blade decreases from the first stage to the fifth stage while inlet angle of blade in each stage is constant. Thus, the incident angle increases along the flow direction, which leading to the increment of energy loss at the inlet of each stage. It is necessary to modify the inlet angle of each stage. In the following part, the hub ratio of inlet and inlet angle of blade are optimized based on the stage-by-stage design method.

##### 4.1.1 Hub Ratio of Inlet

Hub ratio of inlet is the ratio of inlet impeller hub diameter to shroud diameter, which is shown in Eq. (5). From Table 2, it shows the inlet axial velocity of impeller decreases due to the reduction of volume flow rate along the flow direction in the five-stage pump. Thus, the kinetic energy also decreases and the portion converted to pressure energy is reduced which affect the pump boosting ability. The inlet axial velocity is 3.78m/s at the first stage while it decreases to 3.6m/s in the second stage. In order to obtain sufficient kinetic energy, the axial velocity in the second stage is set to 3.78m/s which is the same as that in the first stage. Based on Eqs (1), (2) and (5), the relationship between hub ratio of inlet  $h_{tr}$  and axial velocity  $V_m$  is shown in Eq. (6).

$$h_{tr} = \frac{d_h}{D_i} \tag{5}$$

$$h_{tr} = \sqrt{1 - \frac{4Q}{\pi V_m D_i^2}} \tag{6}$$

At the inlet of the second stage, the volume flow rate  $Q$  is 91.63 m<sup>3</sup>/h, axial velocity  $V_m$  is 3.78m/s. The impeller shroud diameter  $D_i$  is 135 mm. Then hub ratio of inlet  $h_{tr}$  can be calculated. Its value is 0.724 and the inlet impeller hub diameter in the modified second stage is 98 mm.

##### 4.1.2 Inlet Angle of Blade

In order to reduce the incident flow loss at the inlet of impeller, the inlet angle of blade should be decreased. It is determined according to the variation of flow angle from the first stage to the second stage. The inlet angle of blade at impeller shroud and other positions along the radial direction from hub to shroud can be calculated from Eq. (7).

$$D_i \tan \beta_s = d_h \tan \beta_h = const \tag{7}$$

Where  $\beta_s$  and  $\beta_h$  are the inlet angle at impeller shroud and hub separately. From Fig. 2, the inlet flow angle at impeller shroud of the first stage is 6.78°, it decreases to 6.46° in the second stage. Thus, the inlet angle at impeller shroud is set to 6.8° in the modified second stage. Figure 15 shows the meridional plane of the second stage in the original pump and modified pump. It includes the important geometry parameters of impeller blade and diffuser blade (the tip clearance at the impeller shroud is not shown). The  $z$  axis is the central axis of impeller and diffuser and  $r$  axis represents the radial direction. The outline with solid lines is meridional plane of the original pump. And the dotted lines represent the outline of

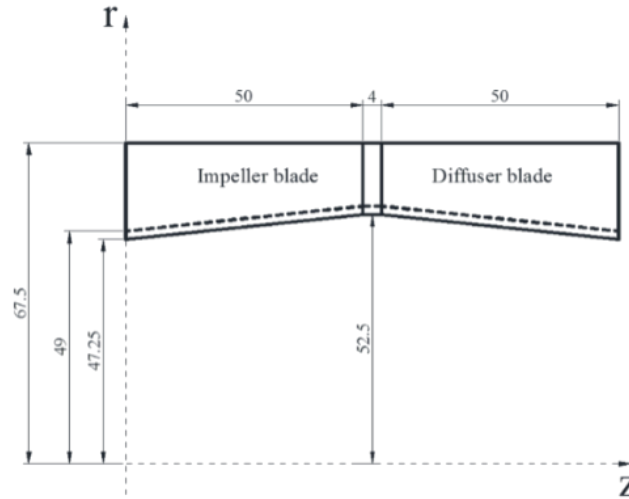


Fig. 15. Meridional plane of the original pump and modified pump.

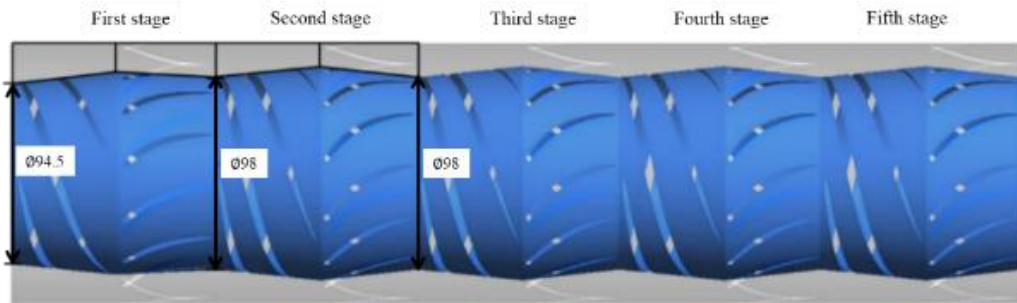


Fig. 16 Outline of the modified five-stage multiphase pump.

the hub of both impeller and diffuser in the modified pump. It clearly shows the reduction of the cross-sectional area of the flow passage in the modified pump. The outline of modified five-stage multiphase pump based on stage-by-stage design method is shown in Fig. 16. The impeller shroud diameters of each stage are the same, while the hub diameter increases from 94.5 mm at the first stage to 98 mm at the second stage. The geometry parameters of remaining stages are the same as the second stage.

#### 4.2 Comparison of Performance Between the Modified Pump and the Original one

Flow parameters and pressure distribution in each stage of the modified five-stage multiphase pump are compared with the original one under the same flow conditions. In the numerical simulation, the rotational speed is 4500 r/min, volume flow rate is 100 m<sup>3</sup>/h and inlet GVF is 30%.

##### 4.2.1 Comparison of the flow Parameters in Each Stage

Figure 17 and Fig. 18 show the comparison of inlet flow rates and flow angles at impeller shroud of each stage in modified pump and original pump separately. In Fig. 17, the inlet volume flow rates from the second stage to the fifth stage of modified pump are lower than those in the original pump. It indicates the compression ability in modified pump

is improved. In Fig. 18, the flow angles at impeller shroud of each stage also increase from the second stage to the fifth stage compare to those of the original pump. Then the incident flow loss can be reduced which contributes to the optimization of flow condition inside the flow passage of impeller.

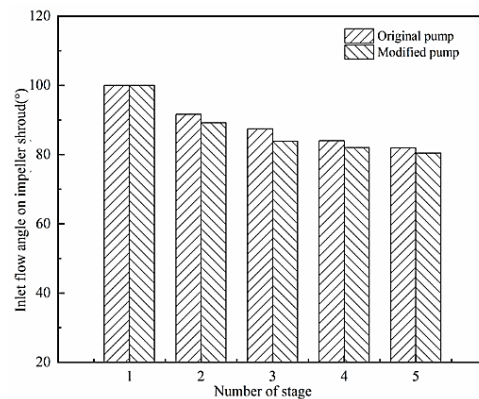
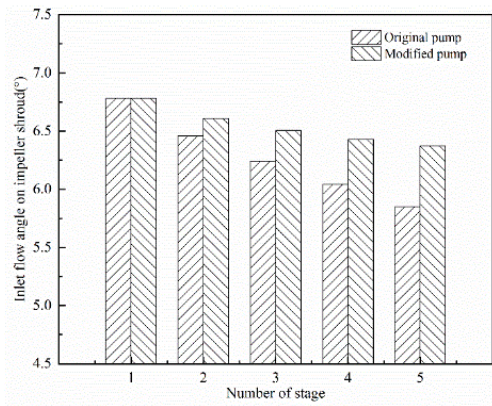


Fig. 17. Comparison of inlet flowrates of each stage in the modified pump and original pump.

##### 4.2.2 Comparison of Pressure Distribution of Each Stage

Comparison of pressure distribution at the leading



**Fig. 18. Comparison of inlet flow angles of each stage in the modified pump and original pump.**

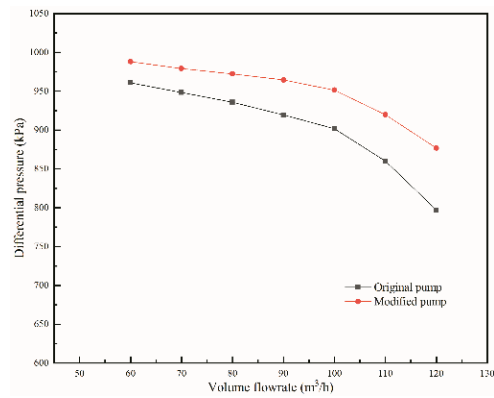


**Fig. 20. Performance comparison between the original pump and modified pump with different volume flowrates ( $n=4500$ r/min,  $GVF=30\%$ ).**

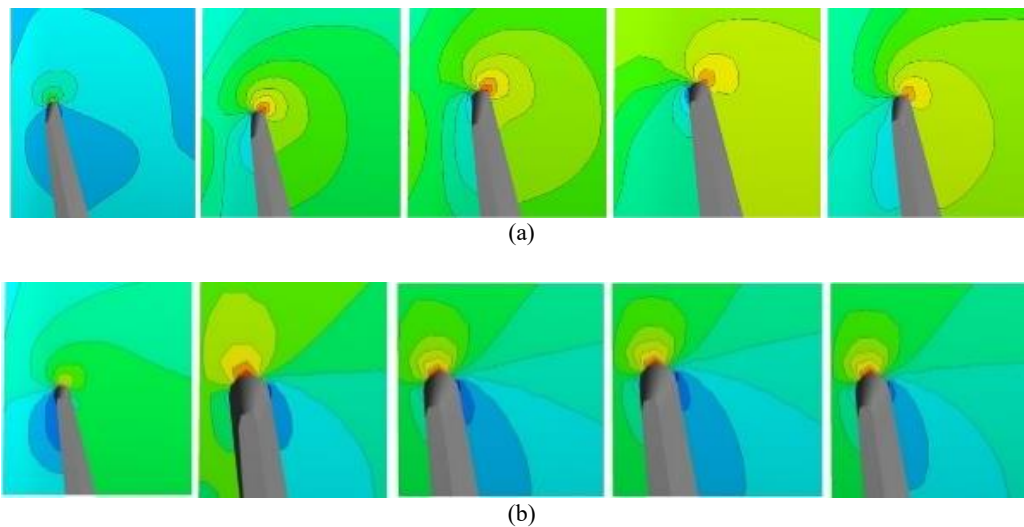


**Fig. 19 Comparison of pressure distribution of each stage at the leading edge of impeller in the modified pump and original pump. (a) Original pump, (b) Modified pump.**

edge of impeller in each stage of modified pump and original pump is shown in Fig. 19. The pressure contours are also shown in this figure. In Fig. 19(a), the five pictures from left to right represent the leading edge on impeller of the first stage to the fifth stage in order. For the first stage, pressure distribution in pressure side and suction side of blade is uniform and the local maximum pressure point occurs at the top point of leading edge in the original pump. But it moves to pressure side of blade from the second stage to the fifth stage, which means there are pressure difference due to large incident flow loss in that area. It is consistent with the conclusion concluded from Fig. 6. Figure 19(b) shows the pressure distribution in modified pump. It becomes uniform in pressure side and suction side at the leading edge from the second stage to the last stage. Local maximum pressure point is also at the top of leading edge. By adjusting the inlet flow angle of blade in each stage to the corresponding flow conditions, the incident flow loss at the leading edge are decreased and the performance is improved as a

result.

The comparison results of flow parameters and pressure distribution in each stage indicate that gas-liquid two-phase flow condition and pump performance have been significantly improved by applying stage-by-stage design method. Figure 20 shows the comparison of the differential pressure between original pump and modified pump with different volume flowrates when the rotational speed is 4500 r/min and inlet GVF is 30%. Since the internal flow conditions have been improved in the modified pump, the whole performance are better than the original one. With the designed condition that volume flow rate is 100 m³/h, rotational speed is 4500 r/min and inlet GVF is 30%, the differential pressure in original pump is 903.64 kPa. It is increased to 957.36 kPa in modified pump. It verifies the feasibility and effectiveness of stage-by-stage design method which based on the corresponding inlet flow conditions in each stage of a multistage multiphase pump.

It should be noted that since the variations of flow parameters such as inlet volume flow rate and flow angle from the second stage to the third stage are not obvious in the modified pump. It is just necessary to modify the second stage while the third stage to the fifth stage are the same as the modified second stage in the aforementioned design flow condition. Actually, the inlet GVF is an important parameter which directly affects the compressibility of gas. According to the research from Zhang *et al.* (2018), when inlet GVF of the pump varies from 10% to 30%, the first two stages should be designed separately and the latter stages are the same as the second stage. So we consider that it is reasonable to just change the second stage. For higher inlet GVFs such as 50%, it is necessary to change more stages in the five-stage pump. The related research will be presented in future's research.

## 5. CONCLUSIONS

A comprehensive investigation on variations of flow parameters in each stage of a five-stage multiphase pump are made based on numerical simulations. Guidelines on the step-by-step design method for a multi-stage multiphase pump are proposed. A five-stage pump is modified based on step-by-step design method in the design conditions. The main conclusions are as follows:

- (1) Numerical simulation method is an effective way to investigate the internal flow characteristics in a multiphase pump. The variations and distribution of flow parameters can be reflected from the numerical simulation results.
- (2) The inlet flow parameters such as volume flow rate and gas volume fraction in each stage decrease along the flow direction in a multi-stage pump which is mainly due to the gas compressibility. Variations of these flow parameters in each stage are easily affected by rotational speed and gas volume fraction. The gas volume fraction and flow angle at impeller shroud vary little as the number of stages increases when inlet GVF is very low (10%) or very high (90%). They vary obviously when inlet GVF ranges from 20% to 80%. Higher rotational speed will contribute to the improvement of pump performance since the gas compressibility is enhanced even in the last few stages of the pump.
- (3) Under the design conditions, the mismatch between inlet flow conditions and geometry parameters at each stage except the first stage in a multistage pump causes the incident flow loss at the leading edge of blade, which also facilitates the deterioration of pump performance. The internal flow condition can be significantly improved by modifying the second stage in a five-stage pump based on the stage-by-stage design method according to corresponding inlet flow parameters. Thereby, the pump boosting capacity is raised. For the design condition with volume flow rate is 100 m<sup>3</sup>/h, rotational speed is 4500 r/min and inlet GVF is 30%, it is just necessary to modified the second stage in the five-stage pump. Further research should be made for higher inlet GVFs on the application of stage-by-stage design method.

## REFERENCES

- ANSYS. (2016). ANSYS Academic Research, Release17, Help System, CFX Documentation. ANSYS, Inc.
- Barrios, L. (2007). *Visualization and modeling of multiphase performance inside an ESP*. PhD thesis, University of Tulsa, Tulsa, USA.
- Barrios, L. J., S. L. Scott and K. K. Sheth (2012, October). ESP technology maturation: subsea boosting system with high GOR and viscous fluid, *SPE Annual Technical Conference and Exhibition*, San Antonio, USA.
- Brennen, C. E. (2011). *Hydrodynamics of pumps*. Cambridge University Press, Cambridge, UK.
- Cirilo, R. (1998). *Air-water flow through electric submersible pumps*. MS thesis, University of Tulsa, Tulsa, USA.
- De Salis, J., C. D. Marolies, J. Falcimaigne and P. Durando (1996, October). Multiphase pumping operation & control. *SPE Annual Technical Conference and Exhibition*, Denver, USA.
- Gamboa, J. (2008). *Prediction of the transition in two-phase performance of an electrical submersible pump*. Phd thesis, University of Tulsa, Tulsa, USA.
- Gié, P. (1992, May). Poseidon multiphase pump: field tests results. *Offshore Technology Conference*, Houston, USA.
- Gülich, J. F. (2014). *Centrifugal pumps*. Springer, Berlin, Germany.
- Mirza, K. Z. and A. G. Wild (1997, October). Key advantages of the progressing cavity pump in multiphase transfer applications. *SPE Annual Technical Conference and Exhibition*, San Antonio, USA, 623-630.
- Nunez, G., J. D. Andrade and M. Stanko (2016). Available technologies and performance prediction models for multiphase booster. *International Conference on Advances in Subsea Engineering. Structures and Systems*, Glasgow, UK.
- Pessoa, R. and M. Prado (2003). Two-phase flow performance for electrical submersible pump stages. *SPE Production & Facilities*, 18(1):13-27.
- Salehi, E., J. Gamboa and M. Prado (2013). Experimental studies on the effect of the number of stages on the performance of an electrical submersible pump in two-phase flow conditions. *WIT Transactions on The Built Environment*.
- Shi, Y., H. W. Zhu and J. Y. Zhang (2017). Investigation of condition parameters in each stage of a three-stage helico-axial multiphase

- pump via numerical simulation. *The 27th International Ocean and Polar Engineering Conference*, California, USA.
- Shi, Y., H. W. Zhu and J. Y. Zhang (2018). Experiment and numerical study of a new generation three-stage multiphase pump. *Journal of Petroleum Science and Engineering*, 169, 471-484.
- Trevisan, F. E. (2009). Modeling and visualization of air and viscous liquid in electrical submersible pump. Phd thesis, University of Tulsa, Tulsa, USA.
- Vetter, G., W. Wirth and H. Korner (2000, March). Multiphase pumping with twin-screw pumps: understand and model hydrodynamics and hydroabrasive wear. *Proceedings of the 17th International Pump Users Symposium*, Houston, USA, 153- 169.
- Zhang, J. and S. Cai (2016). Visualization study of gas-liquid two-phase flow patterns inside a three-stage rotodynamic multiphase pump. *Experimental Thermal & Fluid Science* 70, 125-138.
- Zhang, J., Y. Li and K. Vafai (2018). An investigation of the flow characteristics of multistage multiphase pumps. *International Journal of Numerical Methods for Heat and Fluid Flow* 28(3), 763–784.
- Zhu, J. and H. Q. Zhang (2018a). A review of experiments and modeling of gas-liquid flow in electrical submersible pumps. *Energies* 11, 180.
- Zhu, J., H. Zhu and Z. H. Wang (2018b). Surfactant effect on air/water flow in a multistage electrical submersible pump (ESP). *Experimental Thermal and Fluid Science* 98, 95-111.